Absorption and Emitting Properties of GGG:Ce Single Crystals in the Range of 4f ↔ 5d Transitions of Ce³⁺ Ions

(Proceedings of the Int. Conference on "The Problems of Modern Condensed Matter Physics")

M. Mkrtchyan[1], T. Butaeva[2], A. Eganyan[2,3], K. Ovanesyan[2]

[1]National Scientific Laboratory, 2 Br.Alikhanyan str. 0036 Yerevan, Armenia
[2]Institute for Physical Research, National Academy of Sciences, 0203, Ashtarak-2, Armenia
[3] Armenian State Pedagogical University After Khachatur Abovyan, 13a Khandjyan str., Yerevan, 0010, Armenia
E-mail: mkrtich@mail.yerphi.am

Abstract. The results of a spectral study of both unalloyed and cerium-doped gadolinium-gallium garnet single crystals (GGG and GGG:Ce) are presented.. The effect of the content of activator ions on the absorption properties of these crystals in the region of *4f-5d* transitions of Ce^{3+} ions were considered. Four different photoluminescence bands of Ce^{3+} ions were obtained in a GGG:Ce (*0.1%*) crystal, whose wavelengths are determined by the excitation region of the activator absorption bands. It was shown that the presence of at least four main dodecahedral centers of Ce^{3+} ions in crystals allows one to explain the concentration shift of the activator absorption bands and the mechanism of formation of luminescence bands. Scintillation emission with a maximum at *550 nm* was obtained in GGG:Ce (*0.03* and *0.3%*) crystals upon their excitation by *X*-ray radiation (*22.163 keV*).

1. Introduction

Single crystals of gadolinium gallium garnet GGG ($Gd_3Ga_5O_{12}$) doped with various rare-earths (RE) and transition-metal ions have found wide application in quantum electronics [1], magnetooptics and microelectronics [2], and are also used as phosphors for light-emitting diodes (LED) [3]. Developments in $X-$ or $\gamma-$ray imaging by use of these crystals scintillators for biology, medicine or materials research had been considered in [4]. However, the use of GGG:Ce single crystals as scintillation material remains controversial due to the relatively low emission capacity of the Ce^{3+} ions in these compounds [5, 6]. As noted in [5], these crystals do not show any visible luminescence, since location of the lowest level of the $5d^1$ of Ce^{3+} ion is resonant with the conduction band. Application of hydrostatic pressure ($8\,GPa$) to GGG:Ce crystals allows to restore rather strong luminescence of the Ce^{3+} at $20K$ due to an increase of the crystal band-gap and a simultaneous lowering of the energy of the $4f-5d^1$ transition [6].

GGG crystals are described by structural formula $\{Gd_3\}[Ga_2](Ga_3)O_{12}$, where $\{Gd_3\}$ are ions occupying dodecahedral, $[Ga_2]-$octahedral, and $(Ga_3)-$tetrahedral sites. The crystals production is conjugated with complexities due to high evaporation rate of Ga_2O_3 and their use as the matrix for activator ions is complicated by these crystals own optical activity. The Gd^{3+} ions, being a constituent of the GGG crystal's matrix, participate not only in processes of energy transfer to different defect centers [7], but are themselves luminescence centers at a corresponding excitation of the crystal [8]. For example, the luminescence of uncontrolled impurities of Ce^{3+} and Fe^{3+} ions in this crystal was identified in [7] both upon their direct

excitation and upon transfer of energy from Gd^{3+} ions. The high temperature of the growth of GGG crystals $(\sim 1780C)$ and the presence of two identically charged cations lead to the appearance of "antisite" defects [9], such as Ce_{Al} and Lu_{Al} in $LuAG:Ce$ [10] or Gd_{Ga} in GGG [11]. The noted defects in GGG crystals lead to a change in the lattice parameter, deviations in stoichiometry [12] and the formation of $P-$centers (excited states of RE^{3+} ions located near RE_{Ga}^{3+}) in GGG:RE crystals [11]. Furthermore, the crystals can contain activator ions in a modified valence state, such as Ce^{4+}, like in $YAG:Ce$ [13, 14]. The different types of imperfections located in a vicinity of the dopant (RE^{3+}) of garnet crystals can change the local symmetry and the crystal field strength which leads to the formation of various nonequivalent centers of the activator [15]. The presence of at least two different centers associated with the regular Ce^{3+} along with other (possibly, and Ce_{Ga}) with a lower concentration, in the spectra of the $4f-4f$ transitions of Ce^{3+} ions in GGG:Ce had been discussed in detail in [16].

In this paper we consider the possibility of using single crystals of GGG:Ce for $X-$ray image detectors. The absorption and photoluminescence features of these crystals in the region of $4f-5d$ transition of Ce^{3+} ions are studied taking into account the effect of the activator concentration and the imperfections inherent in these materials. The reasons for the photoinduced change in the absorption bands of Ce^{3+} ions, as well as, unexpectedly for us, and Gd^{3+} ions in GGG:Ce (0.1%) are considered.

2. Experimental

Single crystals of GGG and GGG:Ce were grown by Czochralski method under Ar atmosphere in iridium crucible. The melting point of the crystal flow was $\sim 1780^0 C$. High purity oxides Gd_2O_3, Ga_2O_3, and CeO_2, used as starting row materials, had been previously annealed at $1200^0 C$ for six hours in air. The crystals have been grown from a melt with excess of Ga_2O_3 to compensate evaporation losses. Cerium activated crystals had been grown from the melts containing $0.03-0.3$ at.% of Ce^{3+} ions.

The optical density spectra (D) of GGG crystalline plates with a thickness of $(d)\,0.085cm$ and GGG:Ce with a thickness of 0.075 and $0.2cm$ were recorded in the range $189-900nm$ on a spectrophotometer SPECORD M40 (resolution $\leq 0.1nm$). The luminescence of GGG:Ce (0.1%) crystal excited by halogen lamps "PHILIPS" $(100W)$ was measured at $300K$ on the crystal sample of $0.5\times0.5\times0.8cm^3$ using "DFS-24" spectrometer $(350-800nm)$ with resolving power $\leq 0.01nm$ at $550nm$. Various optical filters were used to change the luminescence excitation range.

Scintillation studies of GGG:Ce crystals $(0.03\text{ and }0.3\%)$ with sizes $1\times1\times0.1cm^3$ were carried out using a device created at the National Science Laboratory (Yerevan, Armenia). The scintillation of these crystals was excited by radiation from an $X-$ray tube with an Ag anode modulated at a frequency of $150Hz$, and the resulting radiation was recorded by a synchronized detector (PMT-85 photomultiplier) and an oscilloscope "Tektronix TDS3054B $(500MHz)$".

3. Results and Discussions

3.1. Transmission and absorption of GGG and GGG:Ce single crystals
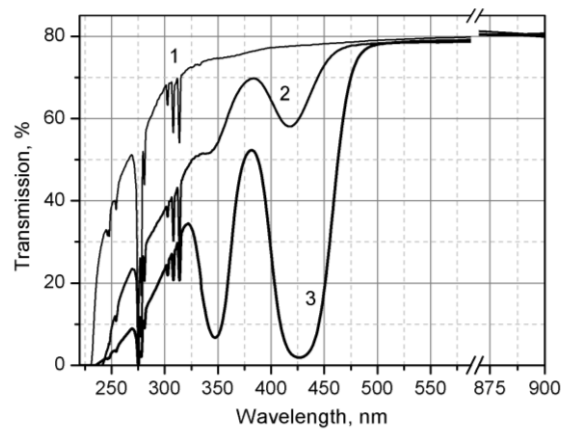
Fig. 1. Transmission spectra of 1 - GGG (*d = 0.075 cm*), 2 - GGG:Ce (0.1 %) (*d = 0.085 cm*), 3 - GGG:Ce (0.2 %) (*d = 0.2 cm*) crystals

Transparency of GGG single crystals allows to successfully activating them with Ce^{3+} ions emitting in the range of $4f \rightarrow 5d$ transitions at $\sim 550nm$. As shown in Fig. 1, the transmission of GGG in this range reaches $\sim 80\%$ and almost does not change in GGG:Ce crystals of various thicknesses.

The absorption spectrum of GGG in the range $190 - 900nm$ (Fig. 2a) shows the UV-absorption edge of this crystal at $\sim 230nm$. The absorption of the color centers characteristic of this compound is shown in Fig. 2 b, c. In compliance with data of [7, 17], the bands at 330 and $350nm$ are due to trapped-hole centers, possibly O^- centers, the bands at $400 - 450nm$, $500nm$ and at $660 - 780nm$ are due to Cr_{oct}^{3+}, Cr_{oct}^{4+} and Cr_{tetra}^{4+}, respectively. Three groups of sharp absorption bands of $4f \rightarrow 4f$ transition of Gd^{3+} ions at $\sim 250, 275$ and $310nm$, corresponding to $^8S \rightarrow {}^6P, {}^6I, {}^6D$ transitions are presented in Fig. 2d. Between the absorption of $^8S \rightarrow {}^6D$ and $^8S \rightarrow {}^6I$ transitions the charge-transfer band of Fe^{3+} (265 nm) [7] is located. Shortwave absorption of $^8S \rightarrow {}^6G$ transition of Gd^{3+} at $\sim 204nm$ [18] is not visible because of the crystal's opacity in this range.
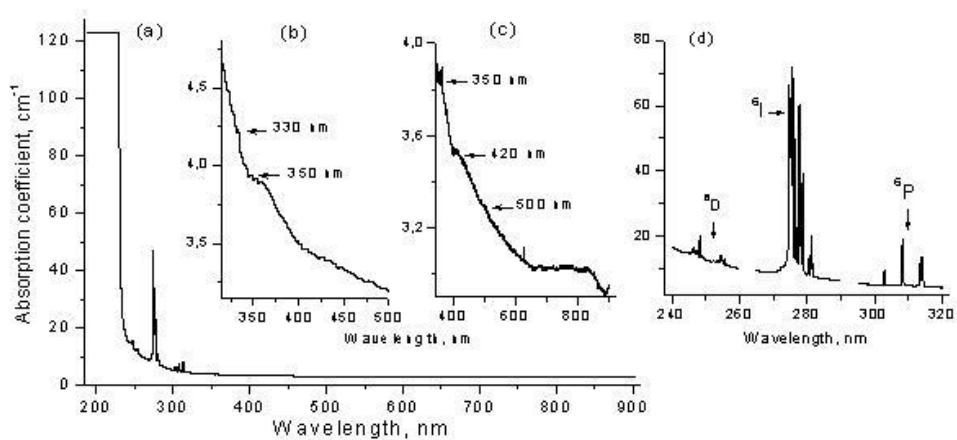
Fig. 2. Absorption of GGG single crystal at: (a) *190-900 nm*, (b) *315 – 500 nm*, (c) *340 -925 nm*, (d) in the range of $^8S \rightarrow {}^6P, {}^6I, {}^6D$ transitions of Gd^{3+} ions.
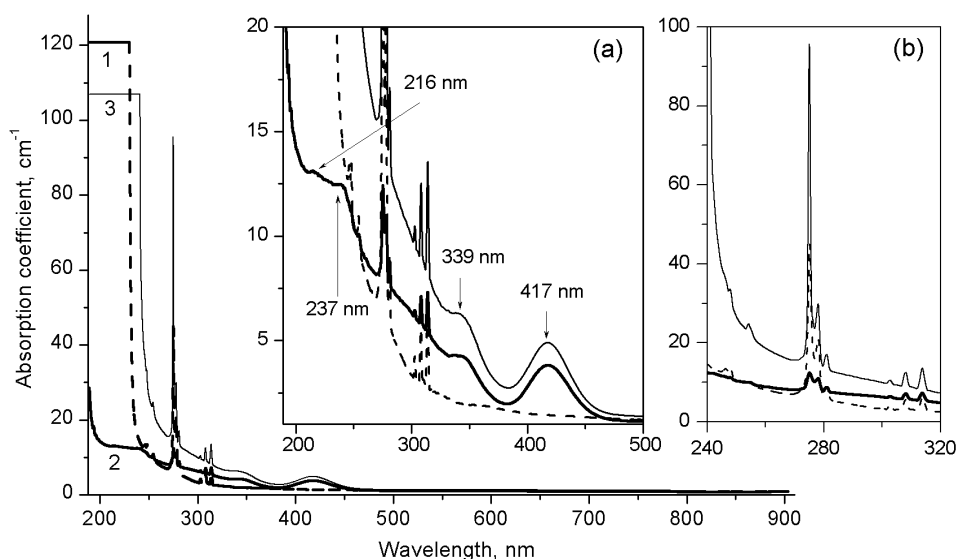
Fig. 3. Absorption of crystals: 1 - GGG (dash line), 2 - as-grown GGG:Ce (*0.1 %*) (bold line) and
3 - GGG:Ce (*0.1 %*) after repeated registration of the spectra (thin line). Insets: zoomed spectra in
the ranges of Ce^{3+} (a) and Gd^{3+} (b) absorption.

Doping of GGG with Ce^{3+} ions (0.1%) leads to a sharp decrease in absorption (Fig. 3, spectrum 2) of the crystal in the UV region (to $189nm$), to the appearance of bands at $216, 237, 339$ and $417nm$ (Fig. 3a) and reduces the intensity of the absorption bands of Gd^{3+} (for example, 1.8 times at $314nm$) compared with an undoped crystal (Fig. 3b, spectrum 1). The long-wavelength absorption bands of Ce^{3+} in GGG: Ce (0.1%) at 339 and $417nm$ [6, 16] overlap with the absorption of color centers at 350 and $420nm$ ((Fig. 2, b, c). And the bands at 216 and $\sim 237nm$ (Fig. 3a), which, according to [16], are in the Ce^{3+} absorption region, are part of a wide continuum of UV-absorption in the region up to $\sim 320nm$, consisting of absorption of Gd^{3+} ions, uncontrolled impurities $Cr^{3,4+}$ and Fe^{3+}, as well as the absorption of F^- and F^+ centers [19, 20].

In contrast to undoped GGG crystal, the repeated registration of GGG:Ce (0.1%) absorption (Fig. 3, spectrum 3) significantly increases UV-absorption of this crystal up to $\sim 240nm$. At the same time, the intensity of the Ce^{3+} bands (at $417nm$) and Gd^{3+} (for example, at $302.8, 308$ and $313.8nm$ of the $^8S \rightarrow ^6P$ transition) sharply rises and almost does not change with subsequent registrations (Fig. 4). The intensity of the absorption band at $417nm$ of Ce^{3+} ions on average increases by 1.302 times, which means the presence of $\sim 30\%$ cerium ions capable of changing the valence state. Thus, the dependences in Fig. 4 can be explained by the presence of Ce^{3+} and Ce^{4+} ions, as well as Gd^{3+} and, possibly, Gd^{2+} ions [21] located near electron or hole traps. As a result, the influence of the radiation from the spectrophotometer source (deuterium lamp) changes the intensity of the Ce^{3+} and Gd^{3+} bands and significantly increases the absorption in the range $190 - 240nm.$ A sharp increase in the absorption of Gd^{3+} ions in the region of the $^8S \rightarrow ^6I$ transition ($\sim 275nm$) after overwriting the absorption spectrum of the

GGG:Ce (0.1%) crystal (Fig. 3b) indicates the possibility of energy transfer between the levels of Fe^{3+}, Cr^{3+} and Gd^{3+} ions, as it was noted in [7].
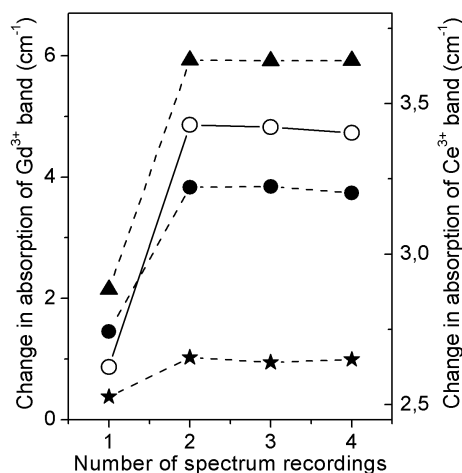
Fig. 4. Change of the intensity of absorption bands:
(left Y-axis) of Gd^{3+} ions (at 302.8 (★), 308 (●), 313.8 (▲) nm; (right Y-axis) of Ce^{3+} ions at *417 (o) nm*
depending on the amount of registration of the absorption spectra of the GGG: Ce crystal (*0.1%*).

3.2. Concentration shift of the absorption bands of Ce^{3+} ions in GGG:Ce single crystals

The increase of the Ce^{3+} concentration to 0.2% in GGG:Ce single crystal, compared with GGG:Ce (0.1%), enhances the intensity of Ce^{3+} absorption bands (Fig. 5), shifts them by $8-9nm$ to the longwave region at 347 and $426nm$ (Fig. 5a), reduces the intensity of the Gd^{3+} bands by ~ 2.5 times and shifts the absorption edge up to $234nm$. Repeated registration of the absorption spectrum of this crystal does not lead to any changes in its absorption. The relative shift of the absorption bands of Ce^{3+} ions in GGG:Ce crystals (Fig. 5a) with a change in the cerium concentration can be explained by the presence of various nonequivalent activator centers, which is typical for crystals with a garnet structure [15]. In this regard, the structure of the bands of Ce^{3+} ions at $417nm$ in GGG:Ce (0.1%) and at $426nm$ in GGG:Ce (0.2%) is considered in more detail.

As shown in fig. 5b, the Ce^{3+} absorption band corresponding to the transition to the lowest energy level $5d^1$ in these crystals can be successfully decomposed into five Gaussian components, designated c_{0-4} for GGG:Ce (0.1%) and c_{1-4} for GGG:Ce (0.2%). It should be noted that the most shortwave components c_0 (at $366nm$) and c_0' (at $187nm$) do not participate in the formation of the main absorption of the Ce^{3+} bands at 417 and $426nm$, but they raise the shortwave wings of these bands by $1.1cm^{-1}$ and $1.6cm^{-1}$, respectively. The band at $366nm$, in accordance with [7], is due to the trapped-hole centers and the band at $187nm$, by analogy with the $YAG:Ce$ crystal [22], can be the result of the formation of an exciton bound to Ce^{3+}. The spectral position and full width at half maximum (FWHM) of the obtained Gaussian components c_{1-4} and c_{1-4}' are presented in Table
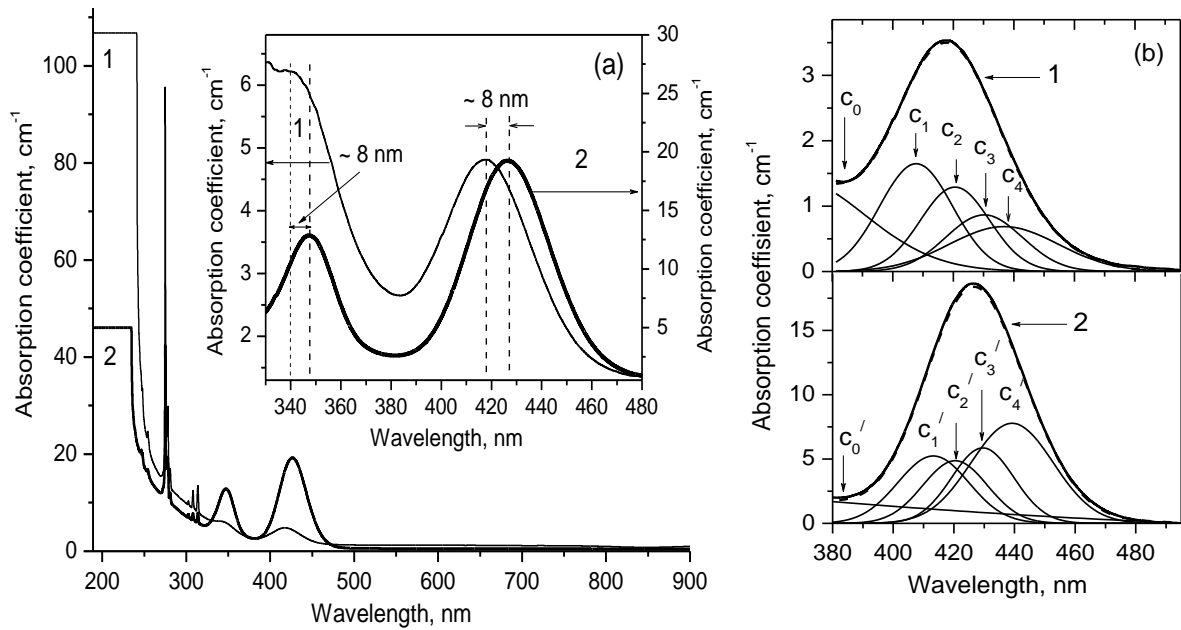
Fig. 5. Absorption of (1) GGG:Ce (*0.1 %*) and (2) GGG:Ce (*0.2 %*) crystals. Insets: (a) – concentration displacement of Ce^{3+} absorption bands; (b) – Gaussian decomposition of the longwave absorption bands of Ce^{3+} (Gaussian absorption components c_{0-4} and c'_{0-4} for the crystals (1) and (2) respectively.

Table 1. Position and FWHM of the longwave absorption band of Ce^{3+} and its Gaussian components in GGG:Ce crystals.

Crystal	Absorption band peak λ (v), nm (cm⁻¹)				FWHM, cm^{-1}			
GGG:Ce (0.1 %)	417 (*23981*)				2667			
	c_1	c_2	c_3	c_4	c_1	c_2	c_3	c_4
	408 (*24510*)	421 (*23753*)	430 (*23256*)	437 (*22883*)	1720	1497	1548	2197
GGG:Ce (0.2 %)	426 (*23474*)				2032			
	c'_1	c'_2	c'_3	c'_4	c'_1	c'_2	c'_3	c'_4
	412 (*24271*)	420 (*23809*)	429 (*23310*)	439 (*22780*)	1627	1393	1333	1598

As follows from Fig. 5b and the data of Table 1, the longwave absorption band of Ce^{3+} includes absorption of at least four centers related to the activator ion. Each of these centers with the corresponding absorption component belongs to Ce^{3+} ion located in one of the four dodecahedral sites with slightly different surrounding due to the presence of the above-

mentioned crystal defects. The close values of the wavelengths of Gaussian components c_{1-4} and c'_{1-4} (Table 1) testify the influence of the same defects on the formation of Ce^{3+} centers in these crystals. But the narrowing of FWHM of Gaussian components $(1.06 \div 1.37$ times) in GGG:Ce (0.2%) compared to GGG:Ce (0.1%) indicates an improvement in quality of the crystal with a higher content of Ce^{3+}. The almost opposite distribution of the absorption intensities of these components with increasing wavelength of their spectral position (a decrease for c_{1-4} and an increase for c'_{1-4}) explains the concentration shift of the absorption peak from $418nm$ in GGG:Ce (0.1%) to $426nm$ in GGG:Ce (0.2%), as seen in Fig. 5b.

3.3. Emitting properties of GGG:Ce crystals

The photoluminescence spectra of $5d \to 4f$ transitions of Ce^{3+} ions in GGG:Ce (0.1%) single crystal, obtained upon excitation of various spectral ranges between $300-600nm$, are shown in Fig. 6a. The energy levels diagram corresponding to the radiative transitions of Ce^{3+} ions is shown in Fig. 6b, where the position of the $5d^1$ levels of GGG: Ce crystals (0.1 and 0.2%) corresponds to the data in Table. 1, and the position of the $^2F_{7/2}$ and $^2F_{5/2}$ levels of the $4f$ configuration is taken from the data [16]. The horizontal dashed lines also indicate the FWHM limits of the lowest and highest levels of the $5d^1$ state. The energy difference between these dashed lines, in fact, determines FWHM of the transitions $5d^1 \to 4f$, in whole. The obtained results are summarized in Table 2.
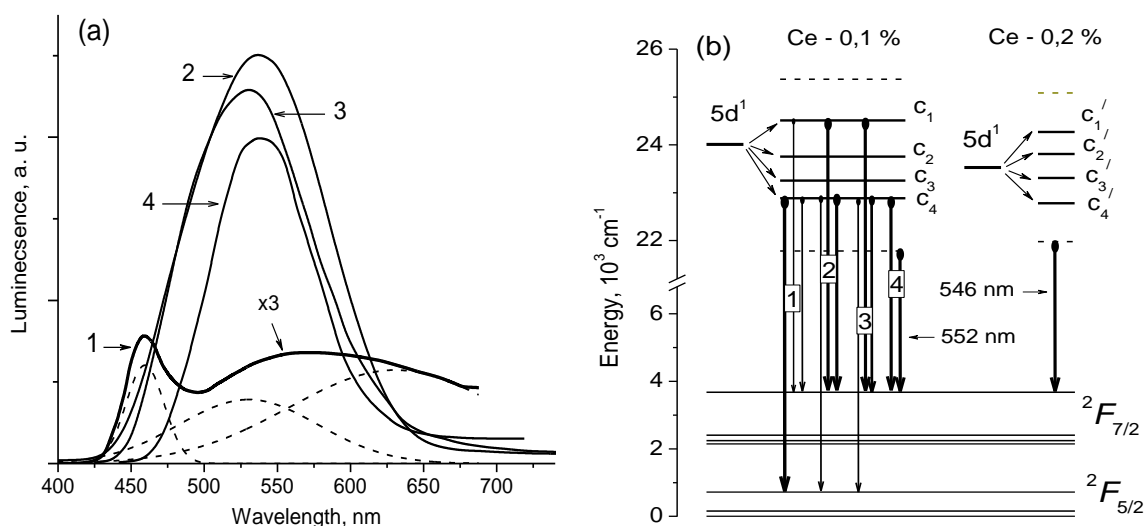
Fig. 6. (a) - photoluminescence spectra $(1-4)$ of GGG:Ce (Ce 0.1 %) excited in different wave ranges: *1 - 300-400 nm, 2 - 360–500 nm, 3 - 360–600 nm* and *4 - 470–600 nm*; (b) - energy structure of the lowest *5d¹* level of *Ce³⁺* in GGG:Ce *(0.1* and *0.2* %) crystals and levels of *4f* levels adduced in [16] (energy levels – solid lines, FWHM of *5d¹* – dash lines).

Table 2. Excitation range and some parameters of Ce^{3+} luminescence obtained in GGG:Ce (*0.1 %*) crystal.

Excitation range, nm	Luminescence peak, nm	FWHM, cm^{-1}	Center	Transition
1. 300 – 400	460.5	1292,3	Ce^{3+}	$c_4\,(5d^1) \rightarrow {}^2F_{5/2}$
	~ 532.6	951.0	Ce^3	$c_{1\text{-}4}\,(5d^1) \rightarrow {}^2F_{7/2}$
	632.4	3668,3	$Ce^{3+}\,(Cr_{oct}^{3+})$	$5d \rightarrow {}^2F_{7/2}\ ({}^2T_1 \rightarrow {}^4A_2)$
2. 360 – 500	~535.2	3815.4	Ce^{3+}	$c_4\,(5d^1) \rightarrow {}^2F_{5/2},$
			Ce^{3+}	$c_{1\text{-}4}\,(5d^1) \rightarrow {}^2F_{7/2}$
3. 360 - 600	529.0	3717.9	Ce^{3+}	$c_4\,(5d^1) \rightarrow {}^2F_{5/2}$
			$(Cr_{oct,tetra}^{3+})$	$c_{1\text{-}4}\,(5d^1) \rightarrow F_{7/2}$
4. 470 – 600	535.5	2867.1	Ce^{3+}	$c_4\,(5d^1) \rightarrow {}^2F_{7/2}$

As it follows from Fig. 6 a, b and Table 2:

- under excitation 1, i.e. in the region of absorption bands of $Gd^{3+}(300-320nm)$, $Ce^{3+}(339nm)$ and the shortwave tail of the Ce^{3+} band at $418nm$, a relatively weak luminescence is observed, consisting of a shortwave narrow band at $460.5nm$ and a broader one that decomposes into two Gaussian components. The narrow band at $460.5nm$ is associated with the transition from the lower component of the $5d^1$ level to the ground state ${}^2F_{5/2}$ (Fig. 6b). The second emission band at $\sim 532.6nm$ is the result of transitions of Ce^{3+} ions from all Gaussian components of the $5d^1$ on the ${}^2F_{7/2}$ state. As for the third band at $\sim 632.4nm$, it can be assumed that this is the radiation of those Ce^{3+} centers that have weak absorption in the region of more than $450nm$. In addition, this is the radiation region of Cr_{oct}^{3+} [7], the absorption band of which is located exactly at $300-400nm$ [17, 23]. But at the present stage of our research, we do not have direct evidence of the latter assumption;

- under excitation 2, i.e. in the range of the absorption bands of Ce^{3+} at $339nm$ and $417nm$, sufficiently intense and broad luminescence band at $535.2nm$ conditioned by the transitions of Ce^{3+} ions is observed;

- under excitation 3, i.e. again in the range of the absorption bands of Ce^{3+} at $339nm$ and $418nm$, the luminescence band conditioned by the same transitions as the luminescence 2, but shifted to the shortwave side at $529nm$ is observed. This displacement can be explained by the narrowing of the luminescence band from the long wave side due to the energy transfer from the Ce^{3+} to Cr_{oct}^{4+} and Cr_{tetra}^{3+} (absorption at $\sim 500-660nm$ [17]) and to Cr_{oct}^{3+} (absorption at $630nm$ [23]);

-under excitation 4, that is, in the region of the long-wave tail of the Ce^{3+} absorption band at $417nm$, the luminescence band is observed at $535.5nm$. The width of this band is noticeably smaller than the width of bands 2 and 3 and is comparable with the absorption band at $417nm$ (Table 3), since in this case only $5d^1 \rightarrow {}^2F_{7/2}$ transitions of Ce^{3+} ions are observed.

Scintillation of GGG:Ce crystals excited by $X-$ ray radiation of $AgK_\alpha (22.163 KeV)$ was detected at $550 nm$ at room temperature. The light yield of these crystals activated with 0.03 and 0.3% of Ce^{3+} ions was 1800 and 23000 ph/MeV, respectively. The result of preliminary measurement of the scintillation decay time in GGG:Ce $(0.3\,at.\%)$ crystal is shown in Fig. 7, where the emission intensity is normalized to 1 and is presented in both linear and logarithmic (inset) scales. Fitting with a first-order exponential function (dashed lines) shows that the decay time in this crystal is $246 ns$. The long time of scintillation decay is most likely due to the presence in these crystals of the multicenter structure of cerium ions with different decay times of each of them. It is expected that more detailed studies of the kinetics of radiation attenuation in these crystals will be published in a separate article.

4. Conclusions

Single crystals of both inactivated GGG and cerium ions activated GGG:Ce were synthesized and peculiarities of their spectral behavior in the range $200-900 nm$ were studied. It was found that a relatively low content (0.1%) of Ce^{3+} ions makes these crystals sufficiently sensitive to UV and visible radiation, in contrast to the photostable GGG and GGG:Ce (0.2%). A photoinduced increase in the intensity of absorption bands of Ce^{3+} ions in GGG:Ce crystal (0.1%) indicates an increased content of electron centers localized about $\sim 30\%$ of the dodecahedral sites of Ce^{4+} ions. A similar photoinduced behavior of the absorption bands of Gd^{3+} ions suggests that some of these centers due to the presence of Gd^{2+} ions in the crystal. An increase in the concentration of Ce^{3+} ions to 0.2% stabilizes the optical quality of these compounds due to an increase in the number of Gd_{Ga} defects that suppress the localization of anion vacancies near the Ce^{3+} dodecahedral site and, accordingly, the ionization of the main Ce^{3+} ions. The concentration shift of the absorption bands of Ce^{3+} ions in crystals containing 0.1 and 0.2% of these ions, as well as the blue and green luminescence of Ce^{3+} ions in GGG:Ce (0.1%) upon excitation of this crystal by UV and visible light, are explained by the formation of a multicenter structure of regular Ce^{3+} ions. The obtained scintillation characteristics of GGG:Ce indicate the possibility of using this material when creating $X-$ ray image detectors.

Acknowledgments

References

[1]   A.A. Kaminskii, V.V. Osiko, S.E. Sarkisov, M.I. Timoshechkin, E.V. Zharikov, J. Bohm, P. Reiche, D. Schultze, J. Appl. Phys., **49** (3) (1978) 1855.
[2]   Young-Duk Huh, Young-Shik Cho, Young Rag Do, Bull. Korean Chem. Soc. **23** (2002) 1435.
[3]   C.W.E. van Eijk, Inorganic scintillators in medical imaging, Phys. Med. Biol., **47** (2002) R85.
[4]   A. Kaminska, A. Duzynska, M. Berkowski, S. Trushkin, and A. Suchocki, Phys.Rev. B, **85** (2012) 155111.1.

[5] I.I. Syvorotka, D.Sugak, A. Wierzbicka, A. Wittlin, H. Przybylińska, J. Barzowska, A. Barcz, M. Berkowski, J. Domagała, S. Mahlik, M. Grinberg, Chong-Geng Ma, M.G. Brik, A. Kamińska, Z.R. Zytkiewicz, A. Suchocki, J. Luminescence, **164** (2015) 31.

[6] G.J. Pogatshnik, L.S. Cain, B.D. Evans, Phys. Rev. B, **43** (1991) 1787-1794.

[7] T. Jenek, K.O. Voss, R. Neumann., K. Schwartz, MATERIALS-09 (GSI, Darmstadt, Germany), p. 317.

[8] M. Nikl, V.V. Laguta, A. Veda, Phys. Stat. Sol. (b), **245** (2008) 1701.

[9] V. Babin, V.V. Laguta, A. Makhov, K. Nejezchleb, M. Nikl, S. Zazubovich, IEEE Transactions on Nuclear Science, **55** (2008) 1156.

[10] M.Kh. Ashurov, Yu.K. Voronko, V.V. Osiko, A.A. Sobol, M.I. Timoshechkin, Phys. Stat. Sol. (a), **42** (1977) 101.

[11] R. Kitamura, Y. Miyazawa, Y. Mori, S. Kimura, J. Crystal Growth, **64** (1983) 207.

[12] S.M. Kaczmarek, G. Domianiak-Dzik, W. Ryba-Romanowski, J. Kisielewski, J. Wojtkowska, Crystal Research and Technology, **34** (1999) 1031.

[13] Yongjun Donga, Guoqing Zhou, Jun Xu, Guangjun Zhao, Fenglian Su, Liangbi Su, Hongjun Li, JiLiang Si, Xiaobo Qian, Xiaoqing Li, Jiong Shen, J. Crystal Growth **286** (2006) 476.

[14] A. Lupei, C. Stoicescu, V. Lupei, J. Cryst. Growth, **177** (1997) 207.

[15] H. Przybylińska, Chong-Geng Ma, M. G. Brik, A. Kamińska, J. Szczepkowski, P. Sybilski, A. Wittlin, M. Berkowski, W. Jastrzębski, and A. Suchocki, Phys. Rev. B, **87** (2013) 045114.

[16] S. Mohamed, S. Jamal, M. Zafer, A.Sh.M. Yassin, Iranian J. Materials Science and Engineering **11** (2014) 79.

[17] R.T. Wegh, H. Donker, A. Meijerink, R.L. Lamminmaki, J. Hölsa, Phys. Rev. B **56** (1997) 13841.

[18] Pujats, M. Springis, Radiation Effects and Defects in Solids, **155** (2001) 65.

[19] T. Butaeva, I. Ghambaryan, M. Mkrtchyan, ISSN 0030-400X, Optics and Spectroscopy, **118** (2015) 247.

[20] E. Malchukova, B. Boizot, D. Ghaleb, G. Petite, J. Non-Crystalline. Solids **352** (2006) 297.

[21] V.A. Andriichuk, L.G. Volzhenskaya, Ya.M. Zakharko, Yu.V. Zorenko, J. Applied Spectroscopy, **47** (1987) 902.

[22] Ya. Zakharko, I.I. Syvorotka, A. Luchechko, I.M. Syvorotka, D. Sugak, M. Vakiv, Acta Physica Polonica A, **117** (2010) 111.